FLOMEKO2019
18th International Flow Measurement Conference
Portugal | Lisbon | LNEC | 26-28 june 2019

Effects of inclination of a clearance-sealed piston prover on the leakage flow rate

G. Bobovnik, J. Kutin

University of Ljubljana, Faculty of Mechanical Engineering, Laboratory of Measurements in Process Engineering, Aškerčeva 6, Ljubljana, Slovenia
E-mail: gregor.bobovnik@fs.uni-lj

Abstract

The leakage flow rate represents one of the most important contributions to the uncertainty of the measured gas flow rate at the bottom limit of the measuring range in a clearance-sealed piston prover. In order to successfully minimize its uncertainty contribution, it is necessary to understand the effects related to the reproducibility of the piston's travelling path relative to the cylinder and to the ability to position the piston prover in the ideal vertical position. The paper deals with an experimental study of the leakage flow rate in the inclined piston prover. The test results show that the leakage flow rate slightly increases with the inclination of the flow cell and that the leakage flow rate is correlated to the pressure inside the flow cell of the piston prover. The results indicate that such relationship could also be applied for predicting the leakage flow rate in a non-inclined piston prover.

1. Introduction

Piston provers are widely used volumetric primary standards in gas flow metering [1-3]. The general principle of operation is based on determining the time interval needed for a piston to pass a known volume of gas at a defined pressure and temperature. The proposed study deals with a clearance-sealed realization of the piston prover, (Figure 1), i.e., the seal in the flow cell is realized by a small clearance of the order of 10 μm between the piston and the cylinder.

The piston prover consists of the base and the flow cell containing the travelling piston. The piston is made of a graphite composite and the cylinder is made of borosilicate glass. The passage of the piston is detected by infrared light emitters and sensors. The flow cell also contains the temperature and gauge pressure sensors that are positioned at the entrance to the cylinder. The base holds the computer, the timebase clock and the barometric pressure sensor. The measurement model for the mass and volume flow rate of the piston prover under study can be expressed as

$$q_{\mathrm{m}} = \rho\left(P_{\mathrm{a}},T\right) q_{\mathrm{v}}\left(P_{\mathrm{a}},T\right),$$
$$q_{\mathrm{v}}\left(P_{\mathrm{a}},T\right) = \left(\frac{V_{\mathrm{m}}^{*}}{\Delta t} + q_{\mathrm{v,l}}\right)\varepsilon_{\rho}, \qquad (1)$$

where $\rho(P_a,T)$ stands for gas density at atmospheric pressure P_a and time-averaged gas temperature in the piston prover T, and V_m^* is the effective measuring volume of the gas collected by the piston prover in the measuring interval Δt. The leakage flow through the clearance between the piston and the cylinder $q_{v,l}$ represents only the Poisseuille component, whereas the Couette component is taken into account when determining the effective measuring volume. The density correction factor ε_ρ [4] accounts for the variations in the density of the gas relative to $\rho(P_a,T)$.

The Poiseuille leakage flow component is driven by a pressure difference on the piston. Considering that the relative pressure difference $\Delta p/P_a$ and the relative piston-cylinder clearance δ/D are relatively small, and that the piston is quiescent in the central position within the cylinder, the Poiseuille leakage volume flow rate can be written as:

$$q_{v,l} = \frac{\pi D \delta^3}{12\mu}\frac{\Delta p}{H} \qquad (2)$$

where D is the piston diameter, H is the piston height and μ is the gas dynamic viscosity. However, the piston position within the cylinder significantly influences the resulting leakage flow rate. For the quiescent piston in its extreme eccentric position,

the Poiseuille leakage volume flow rate is 2.5 times higher than the one resulting from Equation (2). Because the actual travelling position of the piston is unknown, the leakage flow rate has to be determined experimentally.

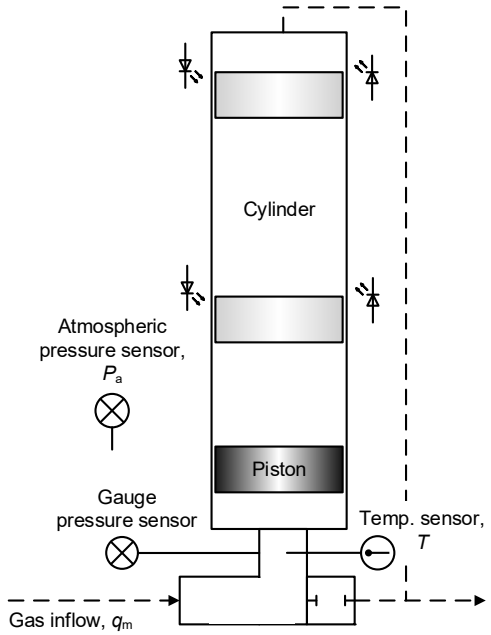

Figure 1: Schematic representation of the piston prover

Our previous study [5] showed that the determination of the leakage flow rate represents one of the most important contributions to the uncertainty of the measured flow rate at the lower limit of the measuring range. In order to successfully minimize its uncertainty contribution, it is vital to understand all important effects contributing to the leakage flow rate. It was presented in [6] that the systematic effects related to the gas viscosity (temperature of the gas, type of the gas) can be successfully corrected. On the other hand, the effects related to the reproducibility of the piston's travelling path relative to the cylinder and to our ability to position the piston prover in the ideal vertical position remain significant. In order to minimize them, the present experimental study focuses on understanding, interpretation and correction of these effects.

The tests with the intention to determine the Poisseuille leakage flow rate and the pressures inside the inclined flow cell were carried out by using the dynamic summation method. Tests were made for different supply air mass flow rates and different inclinations of the piston prover. To ensure that the results are not influenced by viscosity variations the piston prover was placed into a climate chamber, where stable temperature conditions were assured.

2. Measurement method

The dynamic summation method [6] is used to measure the leakage flow rate $q_{v,l}$ during the operation of a piston prover. The gas is supplied from two stable flow sources to two parallel flow branches, each restricted by a valve, which reunite before the inlet to the piston prover. During the measurement the uncorrected readings of the piston prover are recorded by setting $q_{v,l}$ in (1) to zero. So the actual mass flow rate (q_m) is the sum of the uncorrected reading of the piston prover (q_m^*) and the leakage mass flow rate through the piston cylinder clearance ($q_{m,l}$). The mass flow rate is consecutively measured from each flow source separately (q_{m1}, q_{m2}) by closing the valve in the other branch, as well as from both flow sources simultaneously (q_{m1+m2}). By closing a valve in a particular branch the gas is diverted to the surroundings. Assuming that all mass flow rate sources remain stable during the measurement, the following holds true:

$$\begin{aligned} &q^*_{m1+m2} + q_{m,l} = q^*_{m1} + q_{m,l} + q^*_{m2} + q_{m,l} \Rightarrow \\ &q_{m,l} = q^*_{m1+m2} - q^*_{m1} - q^*_{m2}. \end{aligned} \tag{3}$$

Finally, the leakage volume flow rate as defined in the measurement model of the piston prover in Equation (1) is calculated as $q_{v,l} = q_{m,l} / \rho\varepsilon_\rho$, where ρ and ε_ρ are taken as the average values during the measurement.

Using the following sequence of measured flow rates: q_{m1}, q_{m1+m2}, q_{m2}, q_{m1+m2} ..., multiple values of leakage flow rate ($q_{v,l,i}$) are obtained. The mean leakage flow rate and the experimental standard deviation of the mean (ESDM) for N successive measurement results are estimated by [7]:

$$\begin{aligned} q_{v,l} &= \frac{1}{N}\sum_{i=1}^{N} q_{v,l,i}, \\ s\left(q_{v,l}\right) &= \sqrt{\frac{s^2\left(q_{v,l,i}\right)}{N}\left(1 + \frac{2\left(N-1\right)\hat{R}}{N}\right)}, \end{aligned} \tag{4}$$

where $s\left(q_{v,l,i}\right)$ is the experimental standard deviation given by

$$s\left(q_{v,l,i}\right) = \sqrt{\frac{1}{N-1}\sum_{j=1}^{N}\left(q_{v,l,j} - q_{v,l}\right)^2}, \tag{5}$$

and $\hat{R}$ is the sample autocorrelation between the two successive leakage flow rates given by

$$\hat{R} = \frac{\sum_{j=1}^{N-1}\left(q_{v,l,j} - q_{v,l}\right)\left(q_{v,l,j+1} - q_{v,l}\right)}{\sum_{j=1}^{N}\left(q_{v,l,j} - q_{v,l}\right)^2}. \qquad (6)$$

The calculation considers that the two successive leakage flow rates are correlated, because they share one common measured flow rate (q_{m1} or q_{m2}).

3. Measurement system

The leakage flow rate was measured for the piston prover (Sierra Instruments, Cal=Trak SL-800 with flow cell SL-800-10, flow range: 0.0012 g/min to 0.6 g/min). A detailed scheme of the experimental setup is shown in Figure 2.

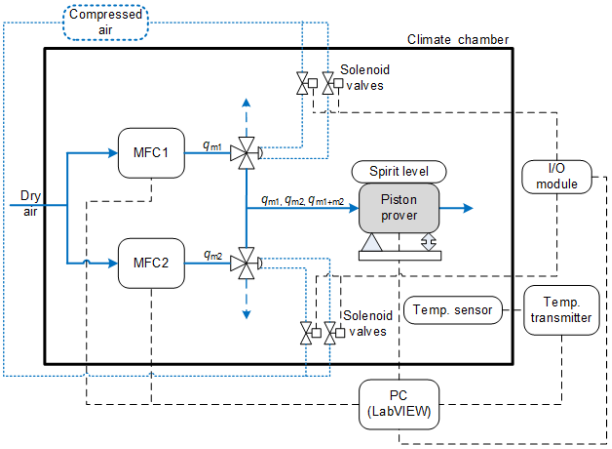

Figure 2: Measuring system

Two mass flow controllers (Bronkhorst F-201CV, full scale value: 13 mg/min) were used for stable flow sources. Downstream of the flow source each branch is restricted by a 3-way valve, enabling the piston prover to measure the flow rate from each source separately or from both sources simultaneously. The 3-way valve is equipped with a double-acting pneumatic actuator, the position of which is controlled using two on/off solenoid valves.

In order to control the temperature conditions and to ensure the temperature stability during the tests, the entire measuring system is placed into a climate chamber (Kambič KK-340 CHLT, stability: 0.1°C). The ambient temperature in the chamber is measured with a Pt100-based measuring system (Tetratec 624T 379 + PicoTech PT-104, expanded uncertainty: 0.15 K). The inclination of the piston prover from vertical is regulated by using the inflatable bellows as schematically shown in Figure 3. The inclination of the piston prover was measured using a digital spirit level (Laserliner, DigiLevel Plus 25, resolution: 0.1°). The adjustment of the inclination was made from outside the chamber and the angle value displayed on the spirit level was monitored by using the camera positioned inside the climate chamber.

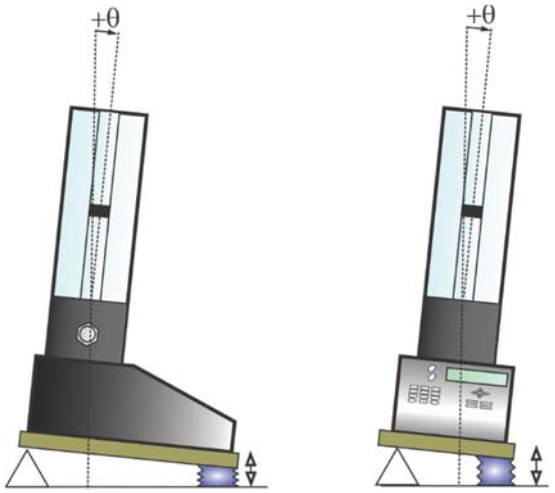

Figure 3: Inclination of the piston prover in the direction of positive angle θ: a) back and forth, b) right and left.

The tests were carried out with dry air. The air properties were calculated using the REFPROP database [8] for a given air temperature in the flow cell and at ambient pressure. Both quantities were measured by using the piston prover's internal sensors, having expanded uncertainties of 0.15 K for the temperature and 0.055 kPa for the ambient pressure. The gauge pressure at the beginning and at the end of the measuring stroke in the flow cell was measured by the integrated pressure sensor having the expanded uncertainty of 1%.

The tests were, with the exception of the inclination adjustment and the temperature regulation of the climate chamber, fully automatized, by using a control program prepared with LabVIEW software (National Instruments, Ver.10.0.).

4. Test results

The tests were carried for different inclinations of the piston prover. The inclination of the piston was changed in two different directions (back and forth, right and left) in the following direction: 0° → 5° → 0° → –5° → 0° in four steps between the indicated values. At the end of the cycle some repetitions were made at random points. The mass flow rate

supplied to the piston was equal to the 50% of the full scale of the mass flow controllers (q_{m1} = q_{m2} ≈ 6.3 mg/min), except for the piston prover's ideal vertical position (0°) at which some measurements were also made at different air supply mass flow rates with mass flow controllers set to 25% and 100% of their full scale. For a single test, the mean leakage flow rate, $q_{v,l}$, and its ESDM, $s(q_{v,l})$, are based on N = 10 consecutively measured values of the leakage flow rate.

During the tests the temperature at the inlet of the piston prover was equal to (22,2 ± 0,1) °C and the ambient pressure was (98,2 ± 0,6) kPa. Hence, the air viscosity changed by less than 0.03% during the experiments.

Figure 4 shows the variation of the leakage flow rate with the angle and the direction of the inclination. The results show a slight increase of the leakage flow rate at higher angles of inclination. The average leakage flow rate at 0° equals about 0.233 ml/min, which is about 23% of the minimum flow rate measured with the flow cell. The standard deviation of the measured values at 0° equals $1.2 \cdot 10^{-3}$ ml/min. The measured leakage flow rates show large scattering for all angles of inclination, which indicates additional influences to the reproducibility of the leakage flow rate, e.g. variations of the piston travelling path, and stability of the mass flow controllers. One can notice that the minimum leakage flow rates are observed at θ of about 1.2°, which could be related to non-alignment of the measuring cylinder inside the flow cell.

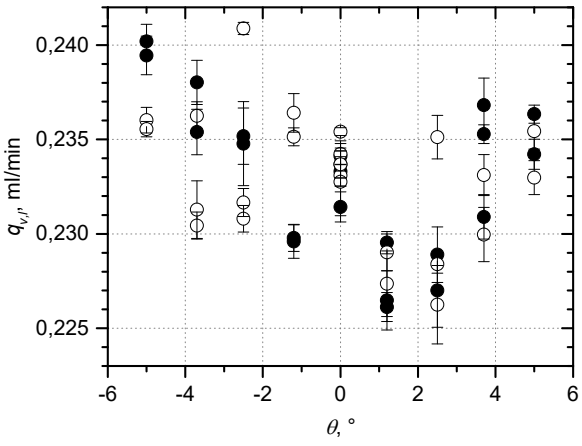

Figure 4: Leakage flow rates at different angles of inclinations of the piston prover (direction: ● - back and forth, ○ - right and left)

To observe if there is any trend of $q_{v,l}$, with the magnitude of inclination, the same data as in Figure 4 are in Figure 5 presented relative to $|\theta|$.

The data show slight increase of the average value of $q_{v,l}$ with $|\theta|$. The linear approximation function predicts an increase in $q_{v,l}$ of about 1.6% for relative change of the inclination of 5°. This estimate is influenced by a large scatter of data and slightly different number of measuring points at each θ.

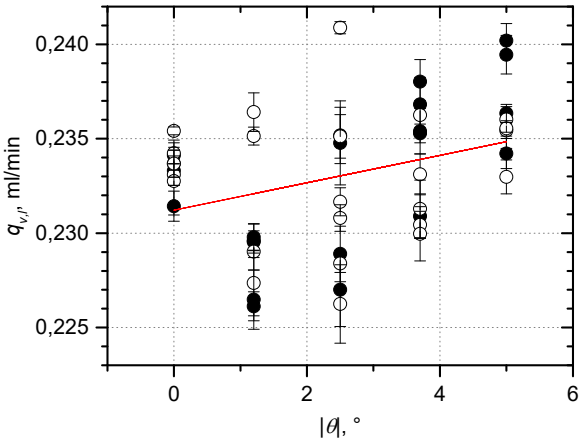

Figure 5: Variation of leakage flow rates for different absolute angles of inclinations of the piston (direction: ● - back and forth, ○ - right and left)

Figures 4 and 5 show that all measured flow rates are within the interval of ±3%, which indicates that the average travelling path of the piston during the measurement stroke remains more or less similar for all measuring points; i.e., note that if the piston travelling path is changed from its central to its extreme eccentric position the leakage flow rate would increase for about 2.5-times. When the flow cell is tilted the most (for 5°) the piston is almost certainly touching the cylinder wall (i.e. sliding along the cylinder wall), which means that it remains in a very similar position also in all other cases.

If we assume that the piston relative position and gas viscosity are relatively constant, then the leakage flow rate could be linked to the variations of the pressure difference acting on the piston. The magnitude of the pressure difference is influenced by the weight of the piston and the friction force acting on the piston. In this case the pressure difference (Δp_θ) at θ relative to the pressure difference (Δp_0) at 0° can be given as:

$$\frac{\Delta p_\theta}{\Delta p_0} = \cos|\theta| + k_f \sin|\theta| , \qquad (7)$$

where the terms on the right-hand of the equation represent the variation of the gravity force and the friction force, respectively. Taking into account that the friction coefficient k_f between the piston and the

cylinder wall is about 0.2 (this value was provided by the manufacturer of the piston-cylinder assembly), the relative increase of pressure for $\theta = 5°$ equals 1.3%, which is close to the estimated increase of the leakage flow rate in Figure 5.

This assumption can be verified by investigating the monitored gauge pressure inside the flow cell. Because the outlet of the flow cell is opened to the ambient, the gauge pressure in the flow cell represents the pressure difference acting on the piston. The integrated sensor does not measure the pressure continuously during the measurement stroke, but only outputs its values at the beginning (p_1) and at the end (p_2) of the stroke.

During the leakage flow test $M = 2N + 1$ individual measurement have to be made to obtain N measurement values of the leakage flow rate (see Section 2). Figure 6 shows the variation of the pressure values $p_{1,i}$, $p_{2,i}$ and their mean value $p_{m,i} = (p_{1,i} + p_{2,i})/2$ for each individual measurement i during the leakage flow test performed at $\theta = 0°$ and $q_{m1} = q_{m2} \approx 6.3$ mg/min. Note that the odd measurements represent pressures obtained for the supplied mass flow rate equal to q_{m1} (or q_{m2}) and the even measurements for $q_{m1+2} \approx 2q_{m1}$. We can see that the pressures change during the test but without influence of the measured mass flow rate. It is also clear that there is no permanent correlation between p_1 and p_2; p_1 can be smaller, grater or equal to p_2 for a given measurement. Therefore, the average (p) of all measured pressures p_1 and p_2 is selected as the pressure parameter characterizing the test:

$$p = \frac{1}{M}\sum_{i=1}^{M}\frac{p_{1,i} + p_{2,i}}{2} \quad , \tag{8}$$

with its experimental standard deviation of mean given by:

$$s(p) = \frac{1}{2}\sqrt{\frac{s^2(p_{1,i}) + s^2(p_{2,i})}{M}} \quad . \tag{9}$$

Figure 7 shows how the mean pressure p changes with the absolute angle of inclination (the results are obtained for the same tests used to measure $q_{v,l}$ in Figures 4 & 5). Despite the relatively large scatter at any given angle of inclination, the increase of the average value of p at higher angles is clearly visible. The linear fit of pressure values predicts the relative change of pressure at 5° of about 1.8%. The results show that the increase of the average pressure in the flow cell is of the same order as the estimated increase of the leakage flow rate. The estimated increase of pressure (leakage flow rate) agrees well with the theoretical prediction from Equation (7).

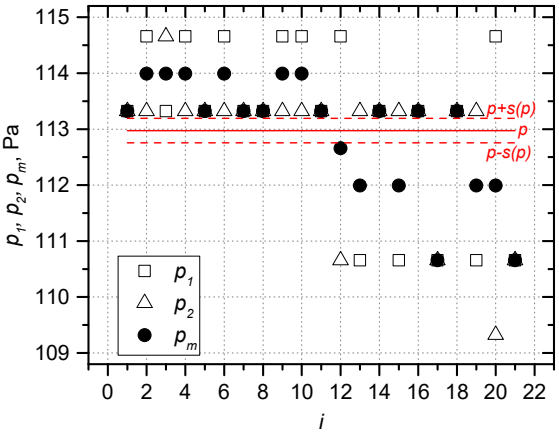

Figure 6: Characteristic pressures p_1, p_2, p_m and p ($\theta = 0°$ and $q_{m1} = q_{m2} \approx 6.3$ mg/min)

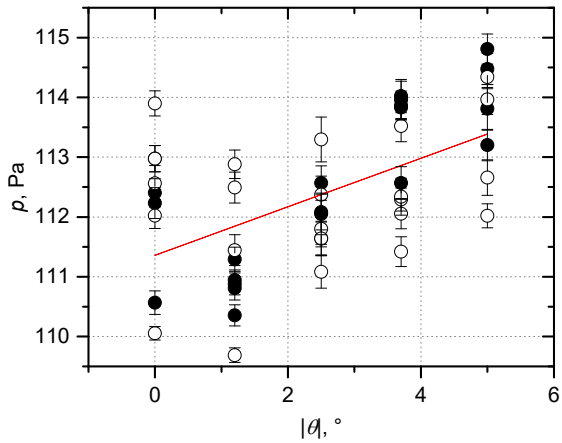

Figure 7: Mean pressures for different absolute angle of inclinations of the piston prover (direction: ● - back and forth, ○ - right and left)

The actual correlation between the leakage flow rate and the mean gauge pressure in the flow cell is presented in Figure 8. The increase of the leakage flow rate with pressure was approximated with linear function, which shows that the ratio $q_{v,l}/p$ remains approximately constant, which confirms our previous observations. Figure 8 also proves some correlation between $q_{v,l}$ and p for a non-inclined flow cell (those results are denoted with black points).

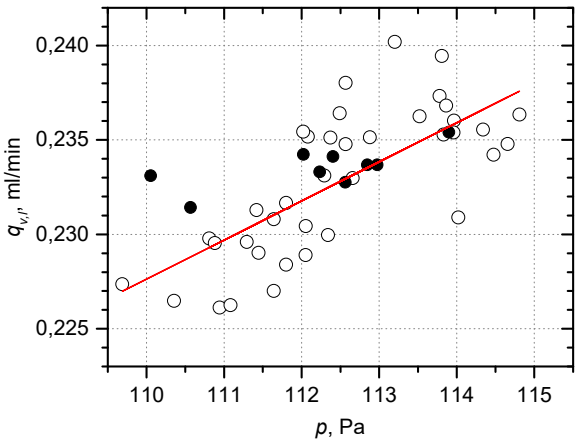

Figure 8: Correlation between the leakage flow rate and the mean pressure (● – measurements at $\theta = 0°$).

7. Conclusion

The presented analysis shows that the leakage flow rate in the inclined clearance-sealed piston prover could be related to the increased friction and therewith to the increased pressure in the flow cell. The results indicate that such relationship could also be used for leakage flow rate prediction in non-inclined flow cell. This would lead to the decrease of the uncertainty of the leakage flow rate related to the repeatability of the travelling path of the cylinder and to the ability to position the flow cell in the ideal vertical position.

The main drawback of the current study is the fact that the pressure inside the flow cell was measured only at the beginning and at the end of the measurement stroke. Monitoring the pressure inside the flow cell during the entire stroke, which would require the use of an external dynamic pressure sensor, would result in a more adequate mean value of the pressure during the measurement stroke. The observed variations of the pressure during the measurement stroke would also provide some additional information about travelling path of the piston.

The tests are also planned for other flow cells with the measuring range up to 50 l/min, in order to research the possibilities of a broader applicability of the current findings.

References

[1] Wright J D, Mattingly G E, Nakao S, Yokoi Y, Takamoto M “International comparison of a NIST primary standard with an NRLM transfer standard for small mass flow rates of nitrogen gas”, *Metrologia*, **35**, 211–221, 1998.

[2] Berg R F, Cignolo G, “NIST–IMGC comparison of gas flows below one litre per minute”, *Metrologia* **40**, 154–158, 2003.

[3] Berg R F, Gooding T, Vest R E “Constant pressure primary flow standard for gas flows from 0.01 cm^3 min^{-1} to 100 cm^3 min^{-1} (0.007–74 µmol s^{-1})”, *Flow Meas. Instrum.,* **35**, 84–91, 2014.

[4] Kutin J, Bobovnik G and Bajsić I, “Dynamic pressure corrections in a clearance-sealed piston prover for gas flow measurements”, *Metrologia*, **50**, 66–72, 2013.

[5] Bobovnik G, Kutin J, Bajsić I “Uncertainty analysis of gas flow measurements using clearance-sealed piston provers in the range from 0.0012 g min^{-1} to 60 g min^{-1}”, *Metrologia*, **53**, 1061–1068, 2016.

[6] Bobovnik G, Kutin J, “Experimental identification and correction of the leakage flow effects in a clearance-sealed piston prover”, *Metrologia*, **53**, 1061–1068, 2016.

[7] Zhang N F, “Calculation of the uncertainty of the mean of autocorrelated measurements”, *Metrologia*, **43**, S276–S281, 2006.

[8] Lemmon E W, Huber M L, McLinden M O, *NIST Reference Fluid Thermodynamic and Transport Properties—REFPROP Version 9.0* (Gaithersburg, MD: National Institute of Standards and Technology), 2010.